LANGMUIR

Article

Cholesterol appended benzimidazolium salts: synthesis, aggregation, sensing, dye adsorption and semiconducting properties

Santanu Panja, Subhratanu Bhattacharya, and Kumaresh Ghosh

Langmuir, **Just Accepted Manuscript** • DOI: 10.1021/acs.langmuir.7b01713 • Publication Date (Web): 30 Jul 2017

Cholesterol appended benzimidazolium salts: synthesis, aggregation, sensing, dye adsorption and semiconducting properties

Santanu Panja, Subhratanu Bhattacharya and Kumaresh Ghosh*

Departments of Chemistry, University of Kalyani, Kalyani-741235, India

ABSTRACT: A series of cholesterol appended benzimidazolium salts **1-9** have been designed and synthesized. They have been explored in gel chemistry. The gelation of the benzimidazolium salts is dependent on the nature of the counter anions. In addition, the gelation behavior of the gelators is linked with the presence of both π-stacking and cholesteryl motifs. While the bisbenzimidazolium salt **2** forms gel in DMSO:H_2O (1:1, v/v) itself, under similar conditions mono benzimidazolium salts **4** and **6** exhibit gelation in the presence of F^- ions and validate the visual sensing of F^-. As application, the gel phase of **2** efficiently removes toxic dyes from waste water. Furthermore, all the gels show thermally activated semiconducting property within a wide voltage window.

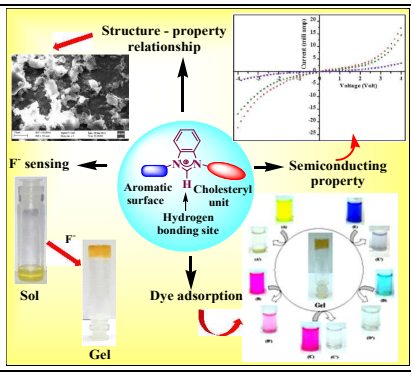

INTRODUCTION

Organic cations such as guanidinium, pyridinium, imidazolium and benzimidazolium etc., are considered to be important binding motifs in devising molecular receptors for recognition and sensing of anionic species.[1-8] The proper placement of these motifs in the designed structures sometime draws attention in supramolecular assemblies and molecules of this class find use in gel chemistry. Gels are considered as viscoelastic solid like materials in which the solvent molecules are entrapped within the gelator molecules to form a three dimensional cross-linked network *via* self-assembly. Different non covalent interactions such as electrostatic, van der Waals, π- stacking and hydrogen bondings play decisive role in this regard.[9-18] Over the last few decades, the interest in supramolecular gels derived from the self-assembly of low molecular weight organic compounds has been increased significantly not only to understand the structure-gelation relationship but also to develop advanced materials with a number of applications in sensing, biomedicine, drug delivery, tissue engineering, photophysics etc.[19-27] In recent years, the development of hydrogels capable of encapsulating pollutants including water soluble toxic dyes has been a focus in material chemistry.[23,28,29]

Of the different charged receptor modules, benzimidazolium-based compounds draw attention due to availability of the polar C-H bond in benzimidazolium motif that takes part in hydrogen bonding with anion and the complex is further stabilized by charge-charge interaction. Careful scrutiny of the literature reveals that a number of synthetic receptors consisting of functionalised benzimidazoles are known in last few years to recognize analytes by accomplishing considerable changes in their absorption and emission spectra during interaction in solution states.[7,30-35] However, the utilization of benzimidazolium moiety in constructing functional gelators for anions is relatively less in number.[36-44] Apart from their use as sensors, the investigation of benzimidazolium-based gelators in dye adsorption process is almost unexplored and therefore, deserves attention.[41-44] It is worthy to be mentioned that dyes are widely used to colour the products in many industries including textile, lather, cosmetics, paper, printing, pharmaceuticals, foods etc. Removal of dyes from waste water is vital as they are toxic to human body and also affect the aquatic ecosystem.[45,46]

Our ongoing interest in the synthesis of stimuli responsive cholesterol-based supramolecular gelators,[36,47-51] has inspired us to report herein the synthesis and gelation behaviour of a series of structurally diversed cholesterol appended benzimidazolium compounds **1-9** (Fig. 1). The gelation of the benzimidazolium salts is dependent on the nature of the counter anion. While the chloride salts exhibit non gelation tendency, the hexafluorophosphate analogues are self assembled either itself or in the presence of externally added anion. In addition, the gelation behavior of the gelators is linked with the presence of both π-stacking and cholesteryl motifs. While the bisbenzimidazolium salt **2** forms gel in DMSO:H_2O (1:1, v/v) itself, under similar conditions mono benzimidazolium

salts **4** and **6** exhibit gelation in the presence of F^- ions and validate the visual sensing of F^-. As application, the gel phase of **2** efficiently removes toxic dyes from waste water. Additionally, each gel shows thermally activated semiconducting property within a wide range of applied voltage.

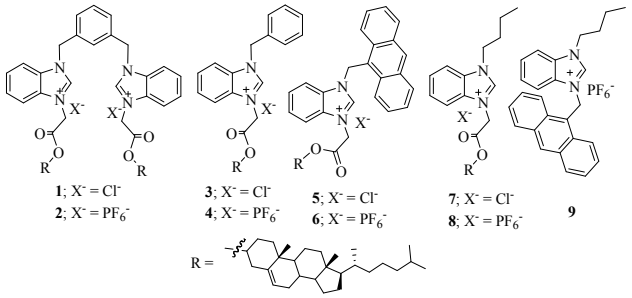

Figure 1. Structures of compounds **1-9**.

RESULTS AND DISCUSSION

Synthesis

Compounds **1-9** were obtained according to the Scheme 1. Cholesterol was initially converted to the chloride **10**.[47] Reaction of benzimidazole separately with *m*-xylene dibromide, benzyl bromide, 9-chloromethyl anthracene and *n*-butyl bromide in the presence of NaH in dry THF afforded compounds **11**,[52] **12**, **13**[53] and **14**, respectively. Salt formation reactions of **11-14** with the chloride compound **10** in dry DMF-CH_3CN produced the chloride salts **1**, **3**, **5** and **7**, respectively. On the other hand, treatment of compound **13** with *n*-butyl bromide under similar conditions

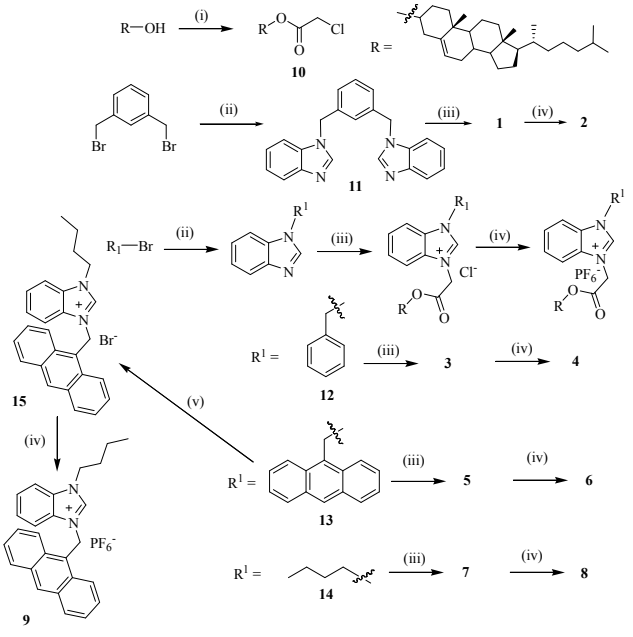

Scheme 1. ((i) chloroacetyl chloride, dry $CHCl_3$, pyridine; (ii) benzimidazole, NaH, dry THF, reflux, 4h; (iii) **10**, dry CH_3CN and DMF, reflux, 3 days; (iv) DMF/CH_3OH, aq. solution of NH_4PF_6; (v) n-butyl bromide, dry CH_3CN and DMF, reflux, 3 days.

gave compound **15**. Anion exchange of **1**, **3**, **5**, **7** and **15** using NH_4PF_6 in aqueous CH_3OH containing 2% DMF afforded the desired compounds **2**, **4**, **6**, **8** and **9**, respectively in appreciable yields. Compounds **1-9** were characterized by usual spectroscopic techniques.

Gelation study, thermal stability and morphologies of gels

In general, in compounds **1-8** the benzimidazolium ring nitrogens are coupled with different substituents of which cholesterol motif is common to all. The supramolecular systems **1** and **2** have been designed based on the $A(LS)_2$ type model in which aromatic benzene ring (A) is connected to the benzimidazolium unit (L), capable of forming hydrogen bonds.[15] Subsequent connection of the cholesterols (S) to the benzimidazoles is considered to maintain a hydrophobic/ hydrophilic balance in the designs. Compounds **3-8** represent ALS-type architectures having different counter anions (Cl^- or PF_6^-) associated with the benzimidazolium functionality. Compounds **1** and **2** are doubly charged whereas the rest of the compounds are mono cationic in nature. The gelation abilities of the compounds **1-9** were examined in different solvents and solvent combinations of different polarities (Table 1S). While compound **1** did not show any gelation ability, compound **2** under similar conditions formed pale yellow colored transparent gel from DMSO–H_2O (1:1, v/v). Use of more water content DMSO (e.g., 25% or 5% DMSO in water) failed to gelate compound **2**. Instead, precipitation appeared due to poor solubility of **2** in such solvent combinations. However, mono cationic gelators **3-9** did not form gel in any of the solvent tested without assistance of any external stimuli. This indicates the key role of more number of cholesterol and benzimidazolium motifs in **2** that trigger the self-aggregation involving hydrogen bonding, π-stacking and hydrophobic interactions.

The hydrogel of **2** exhibited marked stability over four months at room temperature and the gel to sol phase transition temperature (T_{gel}) as determined by capillary insertion method was recorded as 72 °C. The morphology of the gel was characterized by recording the SEM and AFM images. SEM image shows flake like aggregates (Fig. 2a). AFM image also clearly depicts the uneven surface of the gel (Fig. 2b).

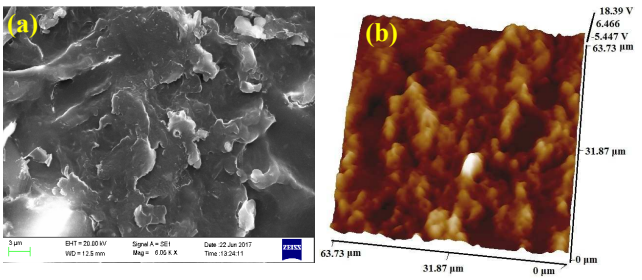

Figure 2. (a) SEM (Scale bar 3 µm) and (b) AFM images of xerogel of **2** from DMSO: H_2O (1:1, v/v).

The inability of **1** in gel formation in comparison to **2** is attributed to the effect of the counter anion. We believe

that the participation of benzimidazolium motif in hydrogen bonding with the chloride ion involving C(2)-H bond does not allow **1** to gelate solvent. Such situation is expected to be absent in **2**. In ^{1}H NMR, the appearance of the signal of benzimidazolium C(2)-H in **1** was noticed in more downfield region compared to the case with **2** and thereby confirmed the hydrogen bonding participation of benzimidazolium motif (Fig. 3A). In FTIR, lowering of stretching frequency of the ester carbonyl of **1** by 7 cm^{-1} with respect to **2** was observed. Beside this, no other characteristic change in the IR spectra like in ^{1}H NMR was worthy to explain the different hydrogen bonding characteristics of bezimidazolium moieties in **1** and **2** (Fig. 1S). In reality, the hydrogen bonding feature of the benzimidazole group with halides is an established fact in the literature.[54-57] Hence, we believe that the molecules of **2** may assume the packing arrangement where interlinking of the molecules produces hydrogen bonded network for solvent trapping to form gel. To get insight in this regard, FTIR spectra of **2** in its amorphous and gel states were compared (Fig. 2S). The signal for ester carbonyl at 1752 cm^{-1} in the amorphous state of **2** underwent shifting to 1743 cm^{-1} in the gel state. This decrease in stretching frequency of the ester carbonyl in **2** is attributed to its involvement in the formation of intermolecular hydrogen bonds during gelation. Moreover, weak π-stacking interactions during aggregation between the aromatic surfaces cannot be ruled out.[36-44]

Benzimidazolium moiety binds anions *via* hydrogen bond involving the C(2)-H bond. In our earlier study, we reported the anion binding behaviour of a similar type of designed molecule in solution phase.[30] To realize more along this direction in gel phase, we explored the gel state of **2** in anion binding by adding aqueous solution of different anions (taken as tetrabutylammonium salts) to the gel of **2** in DMSO/H_2O (1/1, v/v). Of the different anions, only in the presence of NaOH solution, the gel started to collapse and was completely ruptured within five minutes (Fig. 3S). On further acidification, the solution gradually became thick and transformed into gel (Fig. 4S) and thereby indicated its pH responsive behaviour. This pH responsive behaviour is attributed to the acidic nature of the hydrogen in C(2)-H of benzimidazolium motif. In the presence of OH^-, this acidic proton may either be deprotonated or participate in hydrogen bonding due to which the gel state is transformed into the sol state. It is mentionable that the gel is highly stable in the pH range of 2 to 7.8. At higher pH the gel is disintegrated. Fig. 4S represents the pH dependant change of the gel state of **2**. It is to be pointed out that the imidazoliums are unstable in the presence of bases owing to the deprotonation of the acidic C(2)-H to produce N-heterocyclic carbenes (NHC) which undergoes ring-opening reactions in aqueous medium. However, such reactions are highly dependent on the substituents at C(4) and C(5) positions.[58] To investigate the stability of the benzimidazolium salt in the present case, UV-vis and ^{1}H NMR spectra of **2** were recorded in the presence of tetrabutylammonium hydroxide (TBAOH). UV-vis study in DMSO:H_2O revealed no characteristics change in the spectra except at 270 nm where the intensity is gradually decreased due to dilution effect (Fig. 5S). In ^{1}H NMR, the persistence of the C(2)-H signal at 9.78 ppm in the presence of 1 to 2 equiv. amounts of TBAOH suggested non deprotonation (Fig. 6S). In the presence of excess concentration of TBAOH, the deprotonation occurs and it was difficult to interpret by ^{1}H NMR due to significant broadening of the signals.

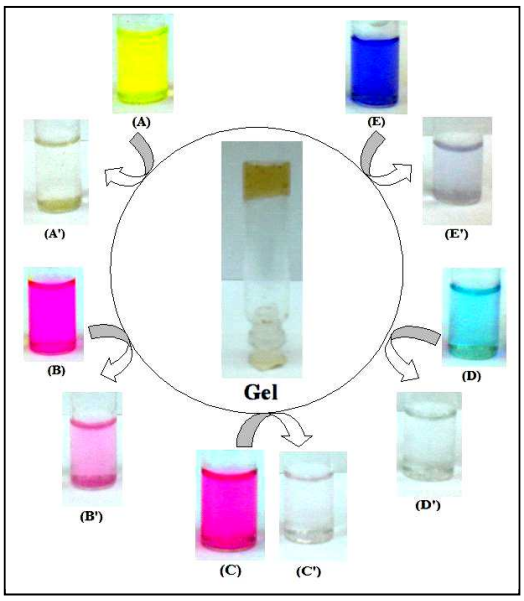

Figure 3. Photograph showing the dye adsorption of Uranine (A→A'), Rhodamine B (B→B'), Rose Bengal (C→C'), Malachite Green (D→D') and Crystal Violet (E→E') (c= 2 x 10^{-5} M) dyes, respectively on keeping in contact with the gel of **2** [8 mg/ml in 1:1 DMSO–H_2O (v/v)] for 24h.

In order to explore the application of gel state of **2**, we used it in dye adsorption. Recently, Thomas *et al.* reported a clay-cross linked hydrogel which can adsorb dyes with opposite charge selectively, and the selective adsorption is based on the electrostatic interaction between the hydrogel and dyes.[59] Experimental findings have intimated that benzimidazolium salts have unique property to adsorb dye molecules from waste water. For such study, both anionic (Uranine, Rhodamine B, Rose Bengal) as well as cationic (Malachite Green, Crystal Violet) dyes were used. The dye adsorption experiment was carried out by monitoring the change in absorbance of the dye solution after keeping in contact with the hydrogel of **2** for 24h. Figure 3 shows the change in color of the dye solutions when they individually remain in contact with the hydrogel of **2**.

A time dependent UV-vis study was performed with 2 mL of corresponding dye solution (in water) (Fig. 7S). As representative example, Fig. 4A corroborates the time dependant change in absorption spectra of the uranine dye when remains in contact with the gel. With time, the absorption maxima of the uranine dye solution was gradually decreased and after 24h it became almost flat without showing any other change in the absorption spectrum. The resulting solution appeared as almost colourless

whereas the gel state acquired the color of the respective dye solutions (Fig. 8S).

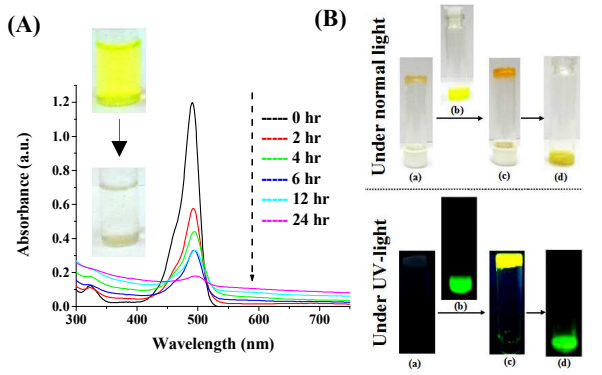

Figure 4. (A) Time-dependent UV–vis spectra of Uranine (c = 2 x 10^{-5} M) solution after keeping in contact with the hydrogel of **2** [8 mg/ml in 1:1 DMSO–H_2O (v/v)]; (B) pictorial representation of the color change of the uranine-adsorbed gel on changing pH: (a) gel of the compound **2** (8 mg/ml) in 1:1 DMSO–H_2O (v/v), (b) aqueous solution of uranine dye (c = 8x10^{-4} M) at pH = 7.2, (c) uranine dye adsorbed hydrogel of **2** at pH = 7.2 and (d) removal of uranine dye from the hydrogel by adding aq. solution of NaOH.

To be confirmed with the adsorption, we further recorded the FTIR spectrum of the gel **2** before and after the adsorption of uranine dye. Adsorption of uranine into the gel matrix resulted in change in stretching frequency of the ester carbonyl groups (Fig. 9S). During adsorption, the morphology of the gel including gel melting temperature (T_g) was changed. The morphology of uranine dye adsorbed gel was observed to be more aggregated in nature than the normal gel (Fig. 9S) and T_g was decreased by 8 °C. In the event the volume of the gel was merely changed.

The pH responsive nature of the dye-adsorbed gel was investigated. Figure 4B represents the effect of aq. NaOH on the uranine dye adsorbed gel of **2** and the associated color changes under ordinary light and UV exposure. While the uranine dye-adsorbed gel shows orange color in ordinary light, the same is viewed as deep yellow under UV illumination. In presence of OH^-, the gel state (pH is checked to be 7.2) is ruptured (pH >8.0) and the original color of dye is retained.

Analysis of dye adsorption experimental findings reveals that the hydrogel of **2** is convincingly capable of removing water pollutant dyes from their aqueous solutions and the dye adsorption capacity of the hydrogel was determined to be 85.3%, 59.9%, 93.6%, 86.0% and 58.2% for Uranine, Rhodamine B, Rose Bengal, Malachite Green and Crystal Violet, respectively (Fig. 5). Table 1 and Fig. 10S represents the details along this direction. It is mentionable that the dye-adsorbed gels were stable over a month. As the adsorption processes and mechanisms are complex, sometime it is difficult to infer proper explanation. However, here we believe that hydrophobic surface as provided by the cholesterol, aromatic surface of the *m*-xylene spacer and the positively charged benzimidazolium motifs altogether play the role in adsorption of the anionic dyes. The hydrogel had almost alike adsorption efficiency towards dianionic dyes Uranine and Rose Bengal whereas it showed relatively much lower adsorption in case of mono

Table 1. Adsorption data of gel **2** using various dyes.

Dye (λ_{max} in nm)	Initial conc. of dye (C_i) [mM] (mgL^{-1})	Equilibrium conc. of dye (C_f) [mM] (mgL^{-1})	Quantity of adsorbed dye (mg per gram of the gelator)
Uranine (490)	2 x 10^{-2} (7.52)	2.94 x 10^{-3} (1.10)	1.60
Rhodamine B (554)	2 x 10^{-2} (9.30)	8.01 x 10^{-3} (3.73)	1.39
Rose Bengal (541)	2 x 10^{-2} (20.30)	1.29 x 10^{-3} (1.31)	4.74
Malachite Green (617)	2 x 10^{-2} (7.28)	2.80 x 10^{-3} (1.01)	1.56
Crystal Violet (590)	2 x 10^{-2} (8.14)	8.36 x 10^{-3} (3.40)	1.18

anionic Rhodamine B. This could be obvious on the basis of the extent of electrostatic interaction between the dicationic hydrogelator molecule and the anionic dyes. The positively charged dyes such as Malachite Green and Crystal Violet in the present study were also significantly captured by the gel. This suggests that the hydrophobicity and π-stacking forces interplay major role over the charge-charge repulsion during dye adsorption. Thus the gel state of **2** is considered to be useful as adsorbent for both anionic and cationic dyes.

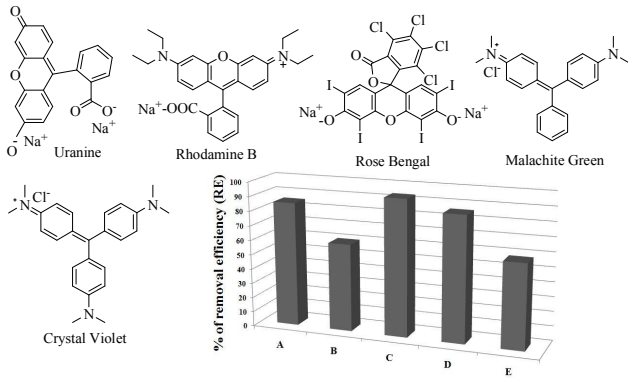

Figure 5. Plot of % of dye removal efficiency (RE) of gel **2** (c = 8 mg/mL) after keeping in contact with the dyes (A = Uranine, B = Rhodamine B, C = Rose Bengal, D = Malachite Green and E = Crystal Violet; [dye] = 2 x 10^{-5} M) for 24h.

In comparison to **2**, mono cationic structures **3-8** behaved differently in gelation. All the compounds **3-8** behaved as nongelator in a number of tested solvents including DMSO: H_2O (1:1, v/v) (Table 1S). However, upon addition of F^- ions, the DMSO: H_2O (1:1, v/v) solutions of **4** and **6** became thick to form pale brown and yellow colored gels, respectively. Under similar conditions, rest of the compounds either resulted in precipitation or exhibited partial gelation. Interestingly, the chloride salt analogues of **4** and **6**, *i.e.* compounds **3** and **5**, respectively, did not exhib-

it gelation. This was most likely due to intramolecular hydrogen bonding of the imidazolium moiety with the closely spaced Cl^- ions that prevents the intermolecular association with the added F^- ions to set up a cross-linked network in solution. In ^{1}H-NMR, more downfield chemical shift of the signals for C(2)-Hs of benzimidazolium moieties in **3** and **5** compared to their hexafluorophosphate analogues **4** and **6**, undoubtedly supports this proposition (Fig. 11S). To our opinion, F^-/HF_2^- (HF_2^- comes from the interaction of F^- with water) ions bind with the benzimidazolium motifs of **4** and **6** in solution involving C(2)-H in the mode as shown in Fig. 12S to set up an aggregation for entrapping solvent.

The hydrogen bonding interaction of F^- with the compounds **4** and **6** was understood from ^{1}H NMR, recorded in $CDCl_3$. As can be seen from Fig. 6, with increase in concentration of F^- ion, the signal for C(2)H_a underwent downfield chemical shift. Moreover, the benzyl protons H_c, in both cases, exhibited downfield chemical shift during interaction (for H_c: $\Delta\delta_4$ = 0.19 ppm and $\Delta\delta_6$ = 0.29 ppm). In this regard, FTIR study of **4** and **6** as shown in Fig. 13S was not informative to interpret the F^- ion interaction.

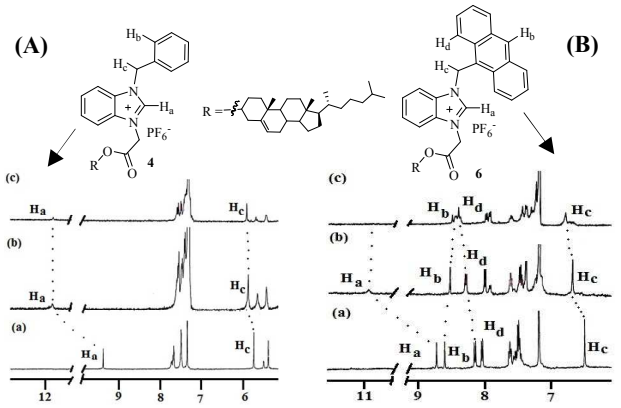

Figure 6. Partial ^{1}H NMR (400 MHz, $CDCl_3$) of compounds (A) **4** (c = 5.50 x 10^{-3} M) and (B) **6** (c = 3.72 x 10^{-3} M) with F^- ion; (a) compound, (b) compound with TBAF (0.5 equiv) and (c) compound with TBAF (1:1).

When the gelation abilities of **7** and **8** in the presence of F^- were examined and compared to that of compounds **4** and **6** under similar conditions, compound **7** resulted in precipitation and **8** showed partial gelation. This observation undoubtedly suggested the subtle role of aromatic stacking in the gel matrices of **4** and **6**. In this regard, for example, absorption and emission spectra of **6** were recorded in solution and gel states to understand the stacking interaction (Fig. 14S). In UV-vis, compound **6** exhibited 3 nm red shifted absorption in gel state. In fluorescence, the broad emission at 498 nm with reduced intensity in the gel state demonstrated the formation of intermolecular excimer/exciplex between anthracenes or anthracene/benzimidazolium moieties. The possible intermolecular hydrogen bonded network as suggested in Fig. 11S gives the emission at longer wavelength due to extensive π-stacking interaction that enhances the scope of intermolecular aggregation during gelation. The aggregation is further stabilized by the hydrophobic interactions exerted by the cholesterol units. The quenching of emission in the gel state is attributed to the 'aggregation-caused quenching' (ACQ) phenomena.[60]

To examine the role of cholesterol unit in the designs, we introduced butyl chain instead of cholesterol in compound **9**. Non gelation behaviour of compound **9** in comparison to **6** strappingly corroborated the crucial role of hydrophobic surface during gelation.

The anion responsive nature of the gelators **4** and **6** was also examined with other anions in details. Except F^-, other anions taken in the study were nonresponsive in bringing sol-gel conversion (Fig. 7a,b). Compounds **4** and **6** at minimum concentrations of 16 mg/mL and 15 mg/mL, respectively, in the presence of 4 equiv. amounts of F^- ions resulted in instant gelation. Use of less than 4 equiv. amounts of F^- ions caused partial gelation in both cases. The fluoride gels of **4** and **6** exhibited thermal induced gel to sol reversible transition and at mgc the gel melting temperatures were recorded to be 58 °C and 62 °C, respectively. The surface morphologies of the gels were studied by SEM images which intimated flake like porous structures (Fig. 7c,d).

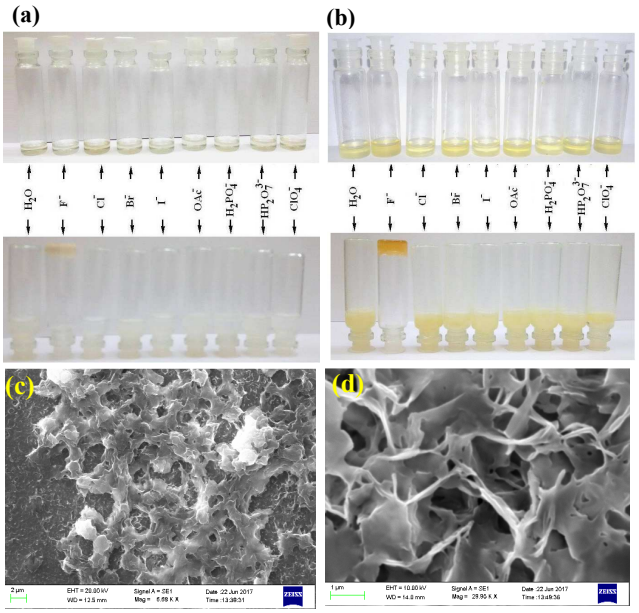

Figure 7. Photographs showing the phase changes of (a) **4** and (b) **6** in DMSO: H_2O (1:1, v/v; 16 mg/ml) upon addition of 4 equiv. amounts of each anion of tetrabutyl ammonium salt (c = 6.2 x 10^{-2} M); SEM images of the xerogels of **4** (c) [Scale bar 2 μm] and **6** (d) [Scale bar 1 μm].

To enquire any role of counter cation during gelation of **4** and **6** with TBAF in DMSO: H_2O (1:1, v/v), similar experiments under identical conditions were performed with KF and CsF. Indeed, all of them induced gelation (Fig. 15S) and hence demonstrated the key role of F^- ion in gelation rather than the counter cation.

To demonstrate the solution phase interactions of **4** and **6** with F^- and other anions in details, fluorescence and UV-vis studies were performed in DMSO-H_2O solvent combi-

nation. In the experiment, compounds were taken in DMSO and aqueous solutions of anionic guests were added to these solutions in different amounts to record the spectra. Although no significant change in the emission of **4** was observed with F^- ions, the absorption spectra reflected significant increase near 340 nm with a clear isosbestic point at 307 nm (Fig. 16S). On the other hand, compound **6** that contains anthracene unit, a well known fluorophore with good quantum yield, exhibited dramatic change in the emission with F^- ions over the other anions taken in the study (Fig. 17S). Initially, on excitation at 370 nm, DMSO solution of **6** showed strong emissions at 400 nm, 422 nm and 448 nm, the characteristic triplet emission of anthracene. On addition of different anionic solutions (in H_2O), small change in emission of **6** was observed except the case with AcO^- and F^- ions. While AcO^- ion resulted in moderate quenching of emission of **6**, under identical conditions F^- ions caused almost complete quenching without producing any other change in emission spectra (Fig. 8a). Fig. 8b in this purpose, represents the change in fluorescence ratio of **6** in the presence of 15 equiv. amounts of different anions. The formation of 1:1 complex of **6** with F^- ion in solution was determined by Benesi-Hildebrand plot[61] from which the association constant value was calculated to be (7.50 ± 0.55) x 10^3 M^{-1} (Fig. 18S).

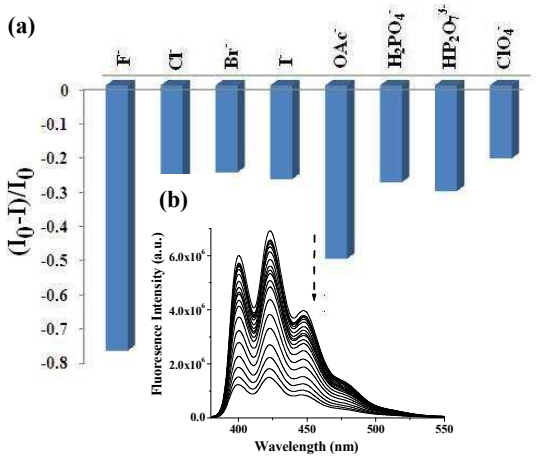

Figure 8. (a) Change in fluorescence ratio of **6** (c = 1.0 x 10^{-5} M in DMSO) at 423nm upon addition of 15 equiv. amounts of anions (c = 4.0 x 10^{-4} M in H_2O); (b) Change in emission of **6** (c = 1.0 x 10^{-5} M) upon addition of 15 equiv. amounts of F^- ion (c = 4.0 x 10^{-4} M).

In ground state, initially **6** displayed structured absorption at 370 nm which gradually increased upon addition of F^- ions. A concomitant decrease in the absorption at 280 nm was recorded (Fig. 19S). Such ratiometric change in the absorption spectra gave isosbestic point at 309 nm. In case of other anions, no significant change was noticed in the absorption spectra of **6** during titration (Fig. 19S).

Current (I)-Voltage (V) characteristics

It has been observed earlier[62,63] that the self-organization of a gelator with π-surface may establish a long-range charge delocalization within the gel matrix, enabling the gel to show semiconducting behaviour. Therefore, we were keen to observe the semiconducting properties of the gels, in addition. This was understood by measuring their temperature dependent current (I)–voltage (V) characteristics as shown in Fig. 9a to Fig. 9c, respectively. Observed symmetric, nonlinear increase in current with increasing voltage in either side clearly demonstrates the semiconducting nature of the gels within the applied voltage range. Moreover, the current gradually increases with temperature showing thermally activated charge transport. The observed semiconducting nature of the gel of **2** presumably arises due to the π- π stacking interaction within the matrix. The gels of **4** and **6** in the presence of F^- show the considerable increase in current (Fig. 9d). This is presumably due to occupancy of anions (either F^- or HF_2^-) in the interstitial positions of the gel networks through hydrogen bonding interactions as shown in Fig. 9. Thus, we believe that the anion doping reinforces the semiconducting property of the gels apparently either by inducing subtle arrangement of the gelators or by increasing charge transfer domains within the gel matrix. As we are aware about the binding of F^- ions involving the imidazolium C(2)-H of compounds **4** and **6** in solution, we believe that such unconventional hydrogen bonding

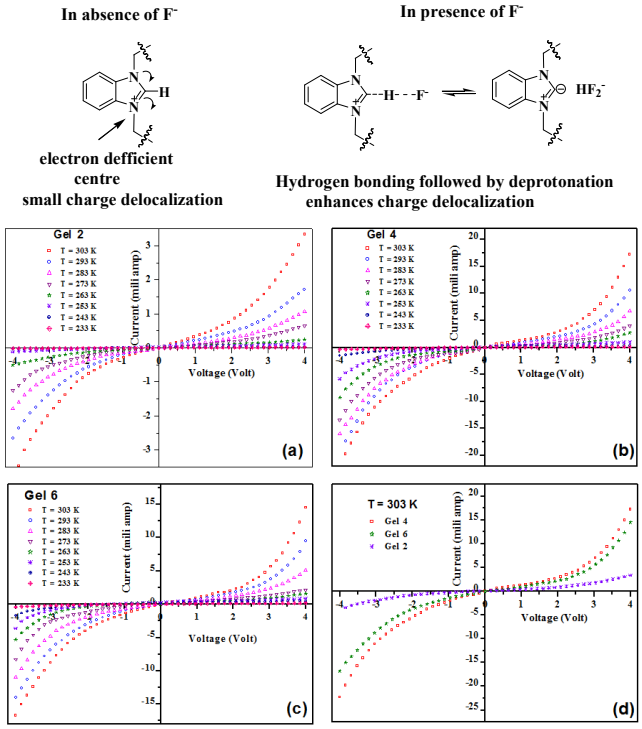

Figure 9. Temperature dependent I–V characteristics of the gels (a) **2**, (b) **4** and (c) **6** (temperature range 233–303 K); (d) Comparison of I-V characteristics of gels **2**, **4** and **6** at room temperature (303 K).

offers the formation of more electronically rich charge centres within the gel phase in comparison to the case of the gel derived from **2**, which intern remarkably enhances the electrical conductivity.

CONCLUSION

In summary, we have designed and synthesized a series of benzimidazolium salts **1-9** that exhibit unique gelation behaviour under different conditions. The gelation of the benzimidazolium salts is dependent on the nature of the counter anions. While the chloride salts exhibit non gelation tendency, the hexafluorophosphate analogues are self assembled either itself or in the presence of externally added anion. Of the different salts, compound **2** itself forms gel in DMSO:H_2O (1:1, v/v), whereas F^- as external anion under similar conditions stimulates the self aggregation of **4** and **6** in aqueous DMSO solvent. This validates the visual sensing of F^-. Rest of the salts behaved as nongelators even in presence of F^- ion. In the designs, the necessity of the aromatic π-stacking and hydrophobic interaction exerted by cholesteryl group has been understood from the structures **8** and **9**.

As application, hydrogelator **2** that possesses more residual charge as well as extensive hydrophobicity due to more cholesterol units was successfully applied as adsorbent of different anionic and cationic dyes. It is experimentally established that the hydrogel of **2** is capable to remove water pollutant dyes from their aqueous solutions and the dye adsorption capacity of the hydrogel has been noted to be 85.3%, 59.9%, 93.6%, 86.0% and 58.2% for Uranine, Rhodamine B, Rose Bengal, Malachite green and Crystal violet, respectively. The dye-adsorbed gels were stable over a month. In addition, all the gels as obtained through different processes, exhibit suitable environment for electron conduction and the observed semiconducting property are thermally activated in nature.

EXPERIMENTAL

Materials

Cholesterol, Chloroacetyl chloride, 9-anthraldehyde, benzyl bromide, butyl bromide and benzimidazole were purchased from Spectrochem. Tetrabutylammonium salts of anions used in the study were purchased from Sigma-Aldrich and were carefully handled. All solvents used in the synthesis were purified, dried and distilled as required. Solvents used in NMR experiments were obtained from Aldrich. Thin layer chromatography was performed on Merck precoated silica gel 60-F_{254} plates. ^1H and ^{13}C NMR spectra were recorded using Bruker 400 MHz instrument using TMS as internal standard. High resolution mass data were acquired by the electron spray ionization (ESI) technique on XEVO GS-2 QTOf Waters mass spectrometer. FTIR measurements of all the compounds and dried gels (xerogels) were carried out using a Perkin-Elmer L120-00A spectrometer (ν_{max} in cm^{-1}) using KBr cell and KBr pellets, respectively. Scanning electron microscopy (SEM) images were obtained on EVO LS-10 ZEISS instrument. Fluorescence and UV-Vis studies were performed using Horiba Fluoromax 4C spectrofluorimeter and Perkin-Elmer LS-55 instruments, respectively.

Synthesis

Chloro-acetic acid 17-(1,5-dimethyl-hexyl)-10,13-dimethyl-2,3,4,7,8,9,10,11,12,13,14,15,16,17-tetradecahydro-1H-cyclopenta[a]phenanthren-3-yl ester (10):[47]

To a stirred solution of cholesterol (0.5 g, 1.29 mmol) in 20 mL dry CH_2Cl_2 was added chloroacetyl chloride (0.16 mL, 1.93mmol) and pyridine (0.05 mL, 0.65 mmol) under nitrogenous atmosphere. The mixture was allowed to stir for 10 h at room temperature. After completion of reaction, the solvent was evaporated and the crude was extracted with $CHCl_3$ (3 × 30 mL). The organic layer was washed several times with water and separated and dried over Na_2SO_4. Evaporation of the solvent gave white solid compound. Recrystallization from petroleum ether afforded pure product **10** (0.58 g, yield 96%), mp 148 °C. ^1H NMR (400 MHz, CDCl3) δ 5.37 (m, 1H), 4.72 (m, 1H), 4.03 (s, 2H), 2.36 (m, 2H), 2.02–0.85 (m, 38H), 0.67 (s, 3H); FTIR (KBr, cm^{-1}): 2939, 2907, 2821, 1753, 1620, 1195.

1, 3-bis ((1H-benzo[d]imdazol-1-yl) methyl) benzene (11):[52]

To a solution of benzimidazole (0.6 g, 5.08 mmol) in dry THF (20 ml), NaH (0.122 g, 5.08 mmol) was added at room temperature. Then the solution was refluxed for 1h. The solution was cooled to room temperature. Then 1, 3-bisbromomethyl benzene (0.67 g, 2.54 mmol) was added to the solution and the reaction mixture was further refluxed for 5h. The solvent was removed under vacuum. Then the reaction mixture was extracted with 50 x 3 ml chloroform containing 2% methanol. The organic solvent was dried over Na_2SO_4 and concentrated under vacuum. The residue was purified by flash column chromatography (ethyl acetate/petroleum ether 80:20, v/v) to afford white crystalline solid compound **11** (0.6 g, yield: 69%), mp 118 °C. ^1H NMR (400 MHz, d_6-DMSO) δ 8.37 (2H, s), 7.66 (2H, d, *J* = 8 Hz), 7.43 (2H, m), 7.26 (1H, t, *J* = 8 Hz), 7.19-7.15 (7H, m), 5.46 (4H, s); ^{13}C NMR (100 MHz, d_6-DMSO) δ 144.1, 143.5, 137.3, 133.5, 129.1, 126.9, 126.8, 122.3, 121.6, 119.4, 110.6, 47.5; FT-IR: ν cm^{-1} (KBr): 3088, 1612, 1496, 1440.

1-(anthracen-9-ylmethyl)-1H-benzo[d]imidazole (13):[53]

To a solution of benzimidazole (0.65 g, 5.50 mmol) in dry THF (25 ml), NaH (0.19 g, 8.26 mmol) was added at room temperature. Then the solution was refluxed for 1h. The solution was cooled to room temperature and 9-chloromethyl anthracene (2.15 g, 9.53 mmol) in 20 mL of dry THF was added to the solution and the reaction mixture was further refluxed for 8h. The solvent was removed under vacuum. Then the reaction mixture was extracted with 5% MeOH in chloroform solution. The organic solvent was dried over anhydrous Na_2SO_4 and concentrated under vacuum. The residue was purified by column chromatography using 30% ethyl acetate in petroleum ether as eluent to afford yellow colored compound **13** in 64% yield (0.79 g). ^1H NMR in CDCl3 (400 MHz) δ 8.61 (s, 2H), 8.10 (d, 4H, J = 8 Hz), 7.82 (d, 1H, J = 8 Hz), 7.71 (d, 1H, J = 8 Hz), 7.51 (m, 4H), 7.42 (t, 1H, J = 8 Hz), 7.35(t, 1H, J = 8 Hz), 6.19 (s, 2H); 13C NMR (CDCl3, 100 MHz) δ 144.0,

142.2, 134.2, 131.4, 131.0, 129.7, 129.5, 127.5, 125.4, 123.6, 123.1, 123.0, 122.5, 120.6, 109.5, 41.3; m/z (ES+): 308.9 [M].

Compound 1:

Compounds **10** (0.41 g, 0.87 mmol) and **11** (0.1 g, 0.29 mmol) were taken in dry CH_3CN (30 mL) containing 1% DMF and the mixture was refluxed for 3 days. The precipitate was filtered off and washed with hot CH_3CN followed by diethyl ether to have the pure dichloride salt **1** in 85% yield (0.32 g), mp 162 °C. ^{1}H NMR (d_6-DMSO, 400 MHz): δ 9.88 (s, 2H), 8.01 (d, 2H, *J* = 8Hz), 7.78 (d, 2H, *J* = 8Hz), 7.65 (t, 2H, *J* = 8 Hz), 7.54-7.51 (m, 5H), 7.38 (s, 1H), 5.83 (s, 4H), 5.57 (s, 4H), 5.33 (s, 2H), 4.59-4.58 (m, 2H), 2.34-0.67 (m, 86H); FTIR (KBr) ν cm^{-1}: 2936, 1745, 1627, 1564; MALDI-TOF-MS: 1192.120 $(M\text{-}2Cl)^+$, 1230.944 $(M\text{-}H+K)^+$.

Compound 2:

The dichloride salt **1** (0.2 g, 0.15 mmol) was dissolved in MeOH (8 mL) containing 2% DMF and an aqueous solution of NH_4PF_6 (0.05 g, 0.3 mmol) was added under hot condition. After stirring the mixture for 30 min, the precipitate was filtered. Repeated crystallization of the precipitate by diethyl ether afforded pure compound **2** in 85% yield (0.2 g), mp 186 °C. ^{1}H NMR (d_6-DMSO, 400 MHz): δ 9.71 (s, 2H), 7.97-7.95 (m, 2H), 7.71 (d, 2H, *J* = 8Hz), 7.61 (m, 1H), 7.59 (t, 2H, *J* = 8 Hz), 7.47 (t, 2H, *J* = 8 Hz), 7.42 (s, 2H), 7.31 (s, 1H), 5.77 (s, 4H), 5.49 (s, 4H), 5.27 (s, 2H), 4.54-4.52 (m, 2H), 2.26-0.67 (m, 86H); ^{13}C NMR (d_6-DMSO, 100 MHz): 166.4, 143.9, 139.4, 135.1, 132.0, 130.6, 130.3, 129.0, 127.8, 127.4, 127.2, 122.9, 114.4, 114.1, 76.1, 56.6, 56.1, 50.2, 49.8, 48.0, 42.3, 38.0, 36.8, 36.5, 36.2, 35.7, 31.7, 28.2, 27.8, 27.7, 24.3, 23.8, 23.0, 22.8, 21.0, 19.3, 18.9, 12.0 (two carbons of the cholesteryl part in the aliphatic region are buried under the signal of d_6-DMSO); FTIR (KBr) ν cm^{-1}: 2951, 1752, 1666, 1571; Mass (HRMS): Calcd. 1192.8673 for $(M\text{-}2PF_6)^+$ found 1192.8738 $(M\text{-}2PF_6)^+$.

Compound 3:

To a solution of benzimidazole (0.75 g, 6.35 mmol) in dry THF (25 ml), NaH (0.22 g, 9.53 mmol) was added at room temperature. Then the solution was refluxed for 1h. The solution was cooled to room temperature. Then benzyl bromide (1.61 g, 9.53 mmol) in 10 mL of dry THF was added to the solution and the reaction mixture was further refluxed for 2h. The solvent was removed under vacuum. Then the reaction mixture was extracted with chloroform. The organic solvent was dried over anhydrous Na_2SO_4 and concentrated under vacuum. The residue was purified by column chromatography using 25% ethyl acetate in petroleum ether as eluent to afford compound **12** in 84% yield (1.11 g). Compound **12** was used directly in the next step.

Compounds **10** (0.33 g, 0.72 mmol) and **12** (0.1 g, 0.48 mmol) were taken in dry CH_3CN (30 mL) containing 1% DMF and the mixture was refluxed for 3 days. The precipitate appeared was filtered off and washed with diethyl ether to have pure chloride salt **3** in 87% yield (0.28 g), mp 184 °C. ^{1}H NMR ($CDCl_3$, 400 MHz): δ 11.88 (s, 1H), 7.65-7.60 (m, 1H), 7.59-7.54 (m, 3H), 7.48-7.46 (m, 2H), 7.43-7.36 (m, 3H), 5.82 (s, 2H), 5.70 (d, 2H, *J* = 4 Hz), 5.40 (d, 1H, *J* = 4 Hz), 4.75-4.72 (m, 1H), 2.40–0.67 (m, 43H); FTIR (KBr) ν cm^{-1}: 1733, 1564, 1456, 1374.

Compound 4:

Compound **3** (0.2 g, 0.29 mmol) was dissolved in MeOH (8 mL) containing 1% DMF and an aqueous solution of NH_4PF_6 (0.09 g, 0.58 mmol) was added under hot condition. After stirring the mixture for 30 min, the precipitate was filtered and washed well with diethyl ether to afford pure compound **4** in 84% yield (0.19 g), mp 172 °C. ^{1}H NMR ($CDCl_3$, 400 MHz): δ 9.34 (s, 1H), 7.67-7.60 (m, 4H), 7.45-7.43 (m, 5H), 5.64 (s, 2H), 5.40 (s, 1H), 5.29 (s, 2H), 4.77-4.72 (m, 1H), 2.39-0.67 (m, 43H); ^{13}C NMR ($CDCl_3$, 100 MHz): 164.9, 142.5, 138.9, 131.8, 131.7, 130.7, 129.5, 129.4, 128.1, 127.6, 127.4, 123.2, 113.7, 113.0, 76.7, 56.6, 56.1, 51.7, 49.9, 47.8, 42.3, 39.7, 39.5, 37.6, 36.8, 36.4, 36.1, 35.8, 31.8, 31.7, 28.2, 28.0, 27.4, 24.2, 23.8, 22.8, 22.5, 21.0, 19.2, 18.7, 11.8; FTIR (KBr) ν cm^{-1}: 2951, 1753, 1570, 1483; HRMS (TOF MS ES+): calcd. 635.4571 $(M\text{-}PF_6)^+$, found 635.4576 $(M\text{-}PF_6)^+$.

Compound 5:

Compounds **10** (0.22 g, 0.48 mmol) and **13** (0.1 g, 0.32 mmol) were mixed in dry CH_3CN (30 mL) containing 5% DMF and the mixture was refluxed for 3 days. Then the solvent was evaporated under reduced pressure and compound **5** was purified by preparative TLC (0.19 g, 77% yield), mp 176 °C. ^{1}H NMR ($CDCl_3$, 400 MHz): δ 11.56 (s, 1H), 8.56 (s, 1H), 8.38 (d, 2H, *J* = 8 Hz), 8.03 (d, 2H, *J* = 8 Hz), 7.65 (t, 2H, *J* = 8 Hz)), 7.53-7.46 (m, 4H), 7.38 (d, 2H, *J* = 4 Hz), 6.77 (s, 2H), 5.57 (d, 1H, *J* = 8 Hz), 5.50 (d, 1H, *J* = 8 Hz), 5.29 (d, 1H, *J* = 4 Hz), 4.63 (m, 1H), 2.29-0.60 (m, 43H); FTIR (KBr) ν cm^{-1}: 2935, 1740, 1623, 1562, 1446; HRMS (TOF MS ES+): calcd. 735.4884 $(M\text{-}Cl^-)^+$, found 735.4890 $(M\text{-}Cl^-)^+$.

Compound 6:

The chloride salt **5** (0.2 g, 0.25 mmol) was dissolved in MeOH (8 mL) containing 3% DMF and an aqueous solution of NH_4PF_6 (0.08 g, 0.5 mmol) was added under hot condition. After stirring the mixture for 30 min, the precipitate was filtered and washed well with diethyl ether to afforded pure compound **6** (0.18 g) in 81% yield, mp 158 °C. ^{1}H NMR ($CDCl_3$, 400 MHz): δ 8.73 (s, 1H), 8.61 (s, 1H), 8.16 (d, 2H, *J* = 8 Hz), 8.05 (d, 2H, *J* = 8H), 7.63 (t, 2H, *J* = 8Hz), 7.57-7.45 (m, 6H), 6.50 (s, 2H), 5.30 (d, 1H, *J* = 8 Hz), 5.24 (d, 1H, *J* = 8 Hz), 5.08 (s, 1H), 4.54-4.52 (m, 1H), 2.89-0.59 (m, 43H); ^{13}C NMR ($CDCl_3$, 100 MHz): 164.7, 142.1, 138.8, 131.9, 131.2, 131.0, 129.7, 129.5, 128.7, 128.4, 127.6, 127.5, 125.7, 123.2, 122.2, 120.0, 113.6, 113.0, 76.7, 56.6, 56.1, 49.9, 47.8, 44.8, 42.2, 39.6, 39.5, 37.6, 36.7, 36.4, 36.1, 35.7, 31.8, 31.7, 28.2, 28.0, 27.3, 24.2, 23.8, 22.8, 22.5, 20.9, 19.2, 18.7, 11.8; FTIR (KBr) ν cm^{-1}: 2952, 1752, 1668, 1559, 1483; HRMS (TOF MS ES+): calcd. 735.4884 $(M\text{-}PF_6)^+$, found 735.4890 $(M\text{-}PF_6)^+$.

Compound 7:

To a solution of benzimidazole (0.58 g, 0.49 mmol) in dry THF (25 ml), NaH (0.17 g, 7.37 mmol) was added at room temperature. Then the solution was refluxed for 1h. The solution was cooled to room temperature and butyl bromide (0.99 g, 7.37 mmol) was added to it. The reaction mixture was further refluxed for 4h. The solvent was removed under vacuum. Then the reaction mixture was extracted with ethyl acetate. The organic solvent was dried over anhydrous Na_2SO_4 and concentrated under vacuum. The residue mass was purified by column chromatography using 20% ethyl acetate in petroleum ether as eluent to afford liquid compound **14** in 78% yield (0.67 g). Compound **14** was used directly in the next step.

Compounds **10** (0.39 g, 0.85 mmol) and **14** (0.1 g, 0.57 mmol) were taken in dry CH_3CN (30 mL) containing 1% DMF and the mixture was refluxed for 3 days. Then the solvent was evaporated under reduced pressure and washed well with diethyl ether to have pure chloride salt **7** in 86% yield (0.31 g), mp 208 °C. ^{1}H NMR ($CDCl_3$, 400 MHz): δ 11.52 (s, 1H), 7.63-7.57 (m, 3H), 7.51-7.48 (m, 1H), 5.65 (d, 2H, *J* = 8 Hz), 5.31 (d, 1H, *J* = 4 Hz), 4.66-4.61 (m, 1H), 4.49 (t, 2H, *J* = 8 Hz), 2.32-0.60 (m, 50H); FTIR (KBr) ν cm^{-1}: 2937, 1747, 1620, 1565, 1226.

Compound 8:

The chloride salt **7** (0.2 g, 0.31 mmol) was dissolved in MeOH (8 mL) and an aqueous solution of NH_4PF_6 (0.1 g, 0.62 mmol) was added under hot condition. After stirring the mixture for 30 min, the precipitate was filtered. Repeated crystallization of the precipitate by diethyl ether afforded pure compound **8** (0.2 g) in 85% yield, mp 162 °C. ^{1}H NMR ($CDCl_3$, 400 MHz): δ 9.27 (s, 1H), 7.77-7.62 (m, 4H), 5.40 (d, 1H, *J* = 4 Hz), 5.28 (s, 2H), 4.75-4.72 (m, 1H), 4.49 (t, 2H, *J* = 8 Hz), 2.42-0.69 (m, 50H); ^{13}C NMR ($CDCl_3$, 100 MHz): 165.0, 142.2, 138.9, 131.7, 130.9, 127.6, 127.4, 123.2, 113.1, 76.7, 56.6, 56.1, 49.9, 47.77, 47.70, 42.3, 39.6, 39.5, 37.7, 36.8, 36.5, 36.1, 35.8, 31.8, 31.7, 30.7, 28.2, 28.0, 27.4, 24.2, 23.8, 22.8, 22.5, 21.0, 19.6, 19.2, 18.7, 13.3, 11.8 (one carbon in the aromatic region is unresolved); FTIR (KBr) ν cm^{-1}: 2945, 1749, 1621, 1573, 1231; HRMS (TOF MS ES+): calcd. 601.4728 $(M\text{-}PF_6)^+$, found 601.4733 $(M\text{-}PF_6)^+$.

Compound 9:

Compound **13** (0.1 g, 0.32 mmol) was dissolved in dry CH_3CN (30 mL) containing 2% DMF and *n*-butyl bromide (0.66 g, 0.48 mmol) was added to it. Then the reaction mixture was refluxed for 3 days. During the course of the reaction, *n*-butyl bromide was added at the time interval of 1 day. After completion of the reaction precipitate appeared was filtered off and washed with hexane to get pure bromide salt **15** in 80% yield (0.11 g). ^{1}H NMR ($CDCl_3$, 400 MHz): δ 11.73 (s, 1H), 8.59 (s, 1H), 8.55 (d, 2H, *J* = 8 Hz), 8.08 (d, 2H, *J* = 8 Hz), 7.72-7.68 (m, 2H), 7.57-7.52 (m, 3H), 7.42 (t, 1H, *J* = 8Hz), 7.17 (t, 1H, *J* = 8 Hz), 6.98 (d, 1H, *J* = 8 Hz), 6.93 (s, 2H), 4.59 (t, 2H, *J* = 8 Hz), 2.05-2.00 (m, 2H), 1.46-1.40 (m, 2H), 1.25 (t, 3H, *J* = 8 Hz).

The bromide salt **15** (0.1 g, 0.22 mmol) was dissolved in MeOH (8 mL) and an aqueous solution of NH_4PF_6 (0.03 g, 0.44 mmol) was added under hot condition. After stirring the mixture for 30 min, the precipitate was filtered and washed well with diethyl ether to afford pure compound **9** (0.09 g) in 84% yield, mp 184 °C. ^{1}H NMR (d_6-DMSO, 400 MHz): δ 9.02 (s, 1H), 8.92 (s, 1H), 8.35 (d, 2H, *J* = 8 Hz), 8.31-8.25 (m, 3H), 8.11 (d, 1H, *J* = 8Hz), 7.82-7.73 (m, 2H), 7.66-7.60 (m, 4H), 6.71 (s, 2H), 4.32 (t, 2H, *J* = 8 Hz), 1.68-1.63 (m, 2H), 1.12-1.07 (m, 2H), 0.75 (t, 3H, *J* = 8 Hz); ^{13}C NMR (d_6-DMSO, 100 MHz): 141.6, 132.2, 131.69, 131.63, 131.4, 130.9, 129.9, 128.8, 127.3, 127.4, 126.1, 123.8, 122.4, 114.7, 114.3, 46.8, 43.8, 31.1, 19.2, 13.6; Mass m/z (ES+): 365.3 $[M\text{-}PF_6]^+$; Anal Calcd for $C_{26}H_{25}F_6N_2P$: C, 61.18; H, 4.94; N, 5.49, Found: C, 61.22; H, 4.98; N, 5.51.

Gelation test and SEM imaging

The respective amounts of compounds **1-9** were dissolved in desired solvents (1 mL) forming a homogeneous solution, slightly warmed and then allowed to cool slowly to room temperature to form a gel. To study the effect of anions, required amount of anionic solutions (in water) were added to the DMSO solution of compounds **1-9**. All the gels were tested by an inversion of vial method. Samples of gels for SEM imaging were dried under vacuum and then coated with a thin layer of gold metal.

AFM measurements:

Atomic Force Microscopy images were recorded under ambient conditions using AFM (Veeco, Innova) operating in the tapping mode. AFM samples were prepared by drop casting a dilute solution of hydro gels on freshly cleaved mica (Ted Pella) and dried cover slip was then put in a vacuum desiccator overnight and the image then analyzed by Veeco SPM Lab Analysis software.

Dye adsorption experiment:

For this study, the gel of **2** [8 mg/ml] was prepared in 1:1 DMSO–H_2O (v/v) solvent. On the top of the gel, 2 mL of aqueous solutions of different dyes (c = 2 x 10^{-5} M) were placed and the solutions were kept undisturbed for 24 h at room temperature. The adsorption of dye during 24 h with various time intervals was monitored by UV-vis study. The removal efficiency (RE) of a dye[64] from its aqueous solution was estimated using UV-vis spectroscopy. The final concentration of the dye in solution was calculated according to the Beer-Lambert law (A = εcl, A is the absorbance of the dye at a certain absorption wavelength in solution, ε is the molar extinction coefficient and l is the path length of the incident light). The molar extinction coefficients of Uranine, Rhodamine B, Rose Bengal, Malachite Green and Crystal Violet dyes in their aqueous solutions were calculated with l = 1.0 cm as 5.97 x 10^4, 9.22 x 10^4, 6.24 x 10^4, 1.27 x 10^4 and 3.12 x 10^4 respectively. The final concentration of the dye in solution could be obtained by the Beer-Lambert equation, which ultimately determined the removal efficiency of the dye *via* the equation as: $RE = (C_i - C_f)/C_i$, in which C_i represents the initial concentration of the dye in solution; C_f is the final concentration of the dye in the presence of adsorbing gel.

General procedure for fluorescence and UV-vis titrations

Stock solution of the compounds **4** and **6** were prepared in DMSO in the concentration of 1.0 x 10^{-5} M. Stock solutions of anions were prepared in H_2O in the concentration of 4.0 x 10^{-4} M. Solution of respective compounds (2 mL) were taken in the cuvette and to this solution different anions were individually added in different amounts. Upon addition, the change in emission of the compounds was recorded. The same stock solutions were used to perform the UV-vis titration experiment in the same way.

I-V measurements

The gel was drop casted on separate cupper electrodes of a cell having gap of 50 μm between them and then allowed to dry in air overnight. The I-V measurement of the cell containing the dried gel was performed under dynamic vacuum by adopting the two probe 4-wire measurement (as shown below) using a Keithely 2400 source meter.

Supporting Information

Gelation results, Time-dependent UV–vis spectra of dyes, emission and absorption spectra, FTIR and ^{1}H NMR spectra, Job plot, binding curves, and copies of ^{1}H, ^{13}C NMR and HRMS.

AUTHOR INFORMATION

Corresponding Author

* Email: *ghosh_k2003@yahoo.co.in*

Notes

The authors declare no competing financial interest.

ACKNOWLEDGMENT

We thank DST, West Bengal, for financial support under the project (sanc. No. 755(Sanc.)/ST/P/S&T/4G-3/2014 dated 27.11.2014). SP thanks CSIR, New Delhi, India for a fellowship.

REFERENCES

(1) Blondeau, P.; Segura, M.; Fernandez, R. P.; de Mendoza, J. Molecular recognition of oxoanions based on guanidinium receptors. *Chem. Soc. Rev*., **2007**, *36*, 198-210.

(2) Schrader, T.; Maue, M. Ammonium, *Amidinium, Guanidinium, and Pyridinium Cation* from Functional Synthetic Receptors, Wiley-VCH Verlag GmbH & Co. KGaA, **2005**, pp: 111–164.

(3) Conley, M. P.; Valero, J.; de Mendoza, J. *Guanidinium-Based Receptors for Oxoanions*. *Supramolecular Chemistry: From Molecules to Nanomaterials*, John Wiley & Sons, **2012**.

(4) Kubik, S. Anion recognition in water. *Chem. Soc. Rev*., **2010**, *39*, 3648-3663.

(5) Ghosh, K.; Sarkar, A. R.; Sarkar, T.; Panja, S.; Kar, D. Progress of 3-aminopyridinium-based synthetic receptors in anion recognition. *RSC Adv*. **2014**, *4*, 20114-20130.

(6) Gilday, L. C.; Robinson, S. W.; Barendt, T. A.; Langton, M. J.; Mullaney, B. R.; Beer, P. D. Halogen Bonding in Supramolecular Chemistry. *Chem. Rev*. **2015**, *115*, 7118-7195.

(7) Molina, P.; Tárraga, A.; Otón, F. Imidazole derivatives: A comprehensive survey of their recognition properties. *Org. Biomol. Chem.*, **2012**, *10*, 1711-1724.

(8) Sessler, J. L.; Gale, P. A.; Cho, W. S. *Anion Receptor Chemistry*, The Royel Society of Chemistry, Cambridge, UK, **2006**.

(9) Fages, F. *Low Molecular Mass Gelators, Topics in Current Chemistry, Springer-Verlag, Berlin*, **2005**, vol. 256, pp. 283.

(10) Smith, D. K. Molecular Gels-Nanostructured Soft Materials, in *Organic Nanostructures*, ed. J. L. Atwood, J.W. Steed, Wiley-VCH, Weinheim, **2008**.

(11) Jones, C. D.; Steed, J. W. Gels with sense: supramolecular materials that respond to heat, light and sound. *Chem. Soc. Rev.*, **2016**, *45*, 6546-6596.

(12) van Esch, J. H.; Feringa, B. L. New Functional Materials Based on Self-Assembling Organogels: From Serendipity towards Design. *Angew. Chem. Int. Ed.* **2000**, *39*, 2263-2266.

(13) Gale, P. A.; Busschaert, N.; Haynes, C. J. E.; Karagiannidis, L. E.; Kirby, I. L. Anion receptor chemistry: highlights from 2011 and 2012. *Chem. Soc. Rev.*, **2014**, *43*, 205-241.

(14) Babu, S. S.; Praveen, V. K.; Ajayaghosh, A. Functional π-Gelators and Their Applications. *Chem. Rev.* **2014**, *114*, 1973-2129.

(15) Svobodova, H.; N.oponen, V.; Kolehmainen, E.; Sievanen, E. Recent advances in steroidal supramolecular gels. *RSC Adv*. **2012**, *2*, 4985-5007.

(16) Vedhanarayanan, B.; Babu, B.; Shaijumon, M. M.; Ajayaghosh, A. Exfoliation of Reduced Graphene Oxide with Self-Assembled π-Gelators for Improved Electrochemical Performance. *ACS Appl. Mater. Interfaces*, **2016**, DOI: 10.1021/acsami.6b09418.

(17) Geiger, C.; Stanescu, M.; Chen, L.; Whitten, D. G. Organogels Resulting from Competing Self-Assembly Units in the Gelator: Structure, Dynamics, and Photophysical Behavior of Gels Formed from Cholesterol–Stilbene and Cholesterol–Squaraine Gelators. *Langmuir* **1999**, *15*, 2241-2245.

(18) Wang, R.; Geiger, C.; Chen, L.; Swanson, B.; Whitten, D. G. Direct Observation of Sol–Gel Conversion: The Role of the Solvent in Organogel Formation. *J. Am. Chem. Soc*. **2000**, *122*, 2399-2400.

(19) Manouras, T.; Vamvakaki, M. Field responsive materials: photo-, electro-, magnetic- and ultrasound-sensitive polymers. *Polym. Chem*., **2017**, *8*, 74-96.

(20) Functional Hybrid Materials, ed. P. G. Romero, C. Sanchez, Wiley-VCH Verlag GmbH & Co. KGaA, Weinheim, **2004**.

(21) Tam, A. Y. Y.; Yam, V. W. W. Recent advances in metallogels. *Chem. Soc. Rev.*, **2013**, *42*, 1540-1567.

(22) Sangeetha, N. M.; Maitra, U. Supramolecular gels: Functions and uses. *Chem. Soc. Rev.*, **2005**, *34*, 821-836.

(23) Bhattacharya, S.; Samanta, S. K. Soft-Nanocomposites of Nanoparticles and Nanocarbons with Supramolecular and Polymer Gels and Their Applications. *Chem. Rev*. **2016**, *116*, 11967-12028.

(24) Busschaert, N.; Caltagirone, C.; Rossomand, W.V.; Gale, P. A. Applications of Supramolecular Anion Recognition. *Chem. Rev.*, **2015**, *115*, 8038-8155.

(25) Zhang, Y.; Kuang, Y.; Gao, Y.; Xu, B. Versatile Small-Molecule Motifs for Self-Assembly in Water and the Formation of Biofunctional Supramolecular Hydrogels. *Langmuir*, **2011**, *27*, 529-537.

(26) Li, Y.; Rodrigues, J.; Toma´s, H. Injectable and biodegradable hydrogels: gelation, biodegradation and biomedical applications. *Chem. Soc. Rev.*, **2012**, *41*, 2193-2221.

(27) Busseron, E.; Ruff, Y.; Moulin, E.; Giuseppone, N. Supramolecular self-assemblies as functional nanomaterials. *Nanoscale,* **2013**, *5*, 7098-7140.

(28) Shen, X.; Zhu, L.; Wang, N.; Y, Lei.; H, Tang. Molecular imprinting for removing highly toxic organic pollutants. *Chem. Commun*., **2012**, *48*, 788-798.

(29) Okesola, B. O.; Smith, D. K. Applying low-molecular weight supramolecular gelators in an environmental setting–self-assembled gels as smart materials for pollutant removal. *Chem. Soc. Rev.*, **2016**, *45*, 4226-4251.

(30) Ghosh, K.; Kar, D.; Sahu, D.; Ganguly, B. Benzimidazolium-based chemosensors: selective recognition of $H_2PO_4^-$, $HP_2O_7^{3-}$, F^- and ATP through fluorescence and gelation studies. *RSC Adv*. **2015**, *5*, 46608-46616.

(31) Kumari, N.; Jha, S.; Bhattacharya, S. olorimetric Probes Based on Anthraimidazolediones for Selective Sensing of Fluoride and Cyanide Ion via Intramolecular Charge Transfer. *J. Org. Chem.*, **2011**, *76*, 8215-8222.

(32) R. Li,; S. Wang, Li, Q.; Lan, H.; Xiao, S.; Li, Y.; Tan, R.; Yi, T. A fluorescent non-conventional organogelator with gelation-assisted piezochromic and fluoride-sensing properties. *Dyes and Pigments*, **2017**, *137*,111-116.

(33) Lee, D. Y.; Singh, N.; Kim, M. J.; Jang, D. O. Chromogenic and Fluorescent Recognition of Iodide with a Benzimidazole-Based Tripodal Receptor. *Org. lett.*, **2011**, *13*, 3024-3027.

(34) Yan, G.; Wu, G.; Qu, W.; Shi, B.; Lin, Q.; Yao, H.; Zhang, Y.; Wei, Taibao, W. A reversible dual-channel chemosensor for fluoride anion. *Supramol. Chem.,* **2015**, *27,* 552–558.

(35) Kaur, N.; Dhaka, G.; Singh, J. Hg^{2+}-induced deprotonation of an anthracene-based chemosensor: set–reset flip-flop at the molecular level using Hg^{2+} and I^- ions. *New J. Chem.,* **2015**, *39*, 6125-6129.

(36) Ma, X.; Zhang, J.; Tang, N.; Wu, J. A thermo-responsive supramolecular organogel: dual luminescence properties and luminescence conversion induced by Cd^{2+}. *Dalton Trans.*, **2014**, *43*, 17236-17239.

(37) Dhinakaran, M. K.; Soundarajan, K.; Das, T. M. Synthesis of novel benzimidazole-carbazole-N-glycosylamines and their self-assembly into nanofibers. *New J. Chem.,* **2014**, *38*, 4371-4379.

(38) Weng, W.; Beck, J. B.; Jamieson, A. M.; Rowan, S. J. Understanding the Mechanism of Gelation and Stimuli-Responsive Nature of a Class of Metallo-Supramolecular Gels. *J. Am. Chem. Soc.* **2006**, *128*, 11663-11672.

(39) Yao, H.; Wu, H. P.; Chang, J.; Lin, Q.; Wei, T. B.; Zhang, Y. M. A carboxylic acid functionalized benzimidazole-based supramolecular gel with multi-stimuli responsive properties. *New J. Chem*., **2016**, *40*, 4940-4944.

(40) Ganta, S.; Chand, D. K. Nanoscale metallogel via self-assembly of self-assembled trinuclear coordination rings: multi-stimuli-responsive soft materials. *Dalton Trans.*, **2015**, *44*, 15181-15188.

(41) Yao, H.; You, X. M.; Lin, Q.; Li, J. J.; Guo, Y.; Wei, T. B.; Zhang, Y. M. Multi-stimuli responsive metal-organic gel of benzimidazol-based ligands with lead nitrate and their use in removal of dyes from waste-water. *Chinese Chem. Lett.*, **2013**, *24*, 703-706.

(42) Dey, A.; Mandal, S. K.; Biradha, K. Metal–organic gels and coordination networks of pyridine-3,5-bis(1-methylbenzimidazole-2-yl) and metal halides: self sustainability, mechano, chemical responsiveness and gas and dye sorptions. *Cryst. Eng. Comm*, **2013**, *15*, 9769-9778.

(43) Zhang, Y. M.; You, X. M.; Yao, H.; Guo, Y.; Zhang, P.; Shi, B. B.; Liu, J.; Lin, Q.; Wei, T. B. A silver-induced metal-organic gel based on biscarboxyl-functionalised benzimidazole derivative: stimuli responsive and dye sorption. *Supramol. Chem.*, **2014**, *26*, 39-47.

(44) Hu, A. B.; Zhou, H.; Pan, Z. Q.; Cheng, Q. R. Hybrid gels of Bis(benzimidazole)-base ligand with perchlorate salts driven by squaric acid: synthesis, characterization and dye adsorption. *J Porous Mater*, **2016**, *23*, 663-669.

(45) Adhikari, B.; Palui, G.; Banerjee, A. Self-assembling tripeptide based hydrogels and their use in removal of dyes from waste-water. *Soft Matter*, **2009**, *5*, 3452-3460.

(46) Chakraborty, P.; Roy, B.; Bairi, P.; Nandi, A. K. Improved mechanical and photophysical properties of chitosan incorporated folic acid gel possessing the characteristics of dye and metal ion absorption. *J. Mater. Chem.*, **2012**, *22*, 20291-20298.

(47) Ghosh, K.; Panja, S. Cholesterol–based Bisamides on Biphenyl Backbone: A Case of Selective Visual Sensing of F^- and $H_2PO_4^-$ through Breaking and Making of Gels. *Chemistry Select*, **2016**, *1*, 3667-3674.

(48) Ghosh, K.; Panja, S. Coumarin-based supramolecular gelator: a case of selective detection of F^- and $HP_2O_7^{3-}$ *RSC Adv.*, **2015**, *5*, 12094-12099.

(49) Ghosh, K.; Panja, A.; Panja, S. Cholesterol appended bis-1,2,3-triazoles as simple supramolecular gelators for the naked eye detection of Ag^+, Cu^{2+} and Hg^{2+} ions. *New. J. Chem*., **2016**, *40*, 3476-3483.

(50) Ghosh, K.; Panja, S. Naphthalene-cholesterol conjugate as simple gelator for selective sensing of CN^- ion. *Supramol. Chem.* **2017**, *29*, 350-359.

(51) Ghosh, K.; Kar, D.; Panja, S.; Bhattacharya, S. Ion conducting cholesterol appended pyridinium bisamide-based gel for the selective detection of Ag^+ and Cl^- ions. *RSC Adv.,* **2014**, *4*, 3798-3803.

(52) Ghosh, K.; Kar, D.; Panja, A.; Petsalakis, I. D.; Theodorakopoulos, G. Benzimidazolium-based new simple ratiometric fluorescent sensor for selective detection of Dihydrogenphosphate. *Supramol. Chem*., **2014**, *26*, 856-863.

(53) Ghosh, K.; Saha, I.; Frohlich, R.; Patra, A. Selective Sensing of Fumarate Over Maleate by Benzimidazolium – Based Fluororeceptors. *Mini-Rev.Org. Chem*. **2011**, *8*, 31-37.

(54) Yoon, J.; Kim, S. K.; Singh, N. J.; Kim, K. S. Imidazolium receptors for the recognition of anions. *Chem. Soc. Rev*., **2006**, *35*, 355-360.

(55) Vickers, M. S.; Beer, P. D. Anion templated assembly of mechanically interlocked structures. *Chem. Soc. Rev.*, **2007**, *36*, 211-225.

(56) Hess, A. E.; Beer, P. D. Chelated charge assisted halogen bonding enhanced halide recognition by a pyridinium-iodotriazolium axle containing [2]rotaxane. *Org. Biomol. Chem.,* **2016**, *14*, 10193-10200.

(57) Caballero, A.; Bennett, S.; Serpella, C. J.; Beer, P. D. Iodoimidazolium salts: halogen bonding in crystals and anion-templated pseudorotaxanes. *CrystEngComm*, **2013**, *15*, 3076-3081.

(58) Wang, B.; Qin, L.; Mu, T.; Xue‖, Z.; Gao, G. *Chem. Rev*., **2017**, DOI:10.1021/acs.chemrev.6b00594.

(59) Thomas, P. C.; Cipriano, B. H.; Raghavan, S. R. Nanoparticle-crosslinked hydrogels as a class of efficient materials for separation and ion exchange. *Soft Matter*, **2011**, *7*, 8192-8197.

(60) Wei, T. –B.; W. –T. Li.; Li, Q.; Su, J. –X.; Qu, W. –J.; Lin, Q.; Yao, H.; Zhang, Y. –M. A turn-on fluorescent chemosensor selectively detects cyanide in pure water and food sample. *Tetrahedron Lett.,* **2016**, *57*, 2767-2771.

(61) Chou, P. T.; Wu, G. R.; Wei, C. Y.; Cheng, C. C.; Chang, C. P.; Hung, F. T. Excited-State Amine–Imine Double Proton Transfer in 7-Azaindoline. *J. Phys. Chem B.* **2000,** *104,* 7818-7829.

(62) Ghosh, K.; Panja, S.; Bhattacharya, S. Naphthalene linked pyridyl urea as a supramolecular gelator: a new insight into naked eye detection of I^- in the gel state with semiconducting behaviour. *RSC Adv*., 2015, **5**, 72772-72779.

(63) Ghosh, K.; Kar, D.; Bhattacharya, S. Fluoride – responsive hydrogel of cholesterol appended pyridinium urea and its metal detecting ability and semi conducting behavior. *Supramol. Chem*. **2014**, *26*, 313-320.
(64) Zhang, X.; Song, J.; Ji, W.; Xu, Ning.; Gao, N.; Zhang, X.; Yu, H. Phase-selective gelators based on closed-chain glucose derivatives: their applications in the removal of dissolved aniline/nitrobenzene, and toxic dyes from contaminated water. *J. Mater. Chem. A,* **2015**, *3*, 18953 – 18962.

GRAPHICAL ABSTRACT

Cholesterol appended benzimidazolium salts: synthesis, aggregation, sensing, dye adsorption and semiconducting properties

Santanu Panja, Subhratanu Bhattacharya and Kumaresh Ghosh*

We report the design, synthesis and gelation behavior of a series of cholesterol linked benzimidazolium salts **1**-**9**. While the bisbenzimidazolium salt **2** forms gel in DMSO:H_2O (1:1, v/v) itself, under similar conditions mono benzimidazolium salts **4** and **6** exhibit gelation in the presence of F^- ions and validate the visual sensing of F^-. As application, the gel phase of **2** efficiently removes toxic dyes from waste water. Furthermore, all the gels show thermally activated semiconducting property within a wide voltage window.